ELSEVIER

Materials Science and Engineering B57 (1998) 40–45

MATERIALS SCIENCE & ENGINEERING B

Infrared dielectric response of the $La_{2/3}TiO_3$–$LaAlO_3$ microwave ceramics system

J. Petzelt [a,*], E. Buixaderas [a], G. Komandin [a,b], A.V. Pronin [a,b], M. Valant [c], D. Suvorov [c]

[a] *Institute of Physics, ASCR, Na Slovance 2, 18221 Praha 8, Czech Republic*
[b] *Institute of General Physics, RAS, Vavilova 38, 117942 Moscow, Russia*
[c] *'Jožef Stefan' Institute, Jamova 39, 1000 Ljubljana, Slovenia*

Received 14 April 1998

Abstract

Room temperature infrared reflectivity and near-millimetre transmission of $(La_{2/3}TiO_3)_{1-x}(LaAlO_3)_x$ (LTA $-$ x) perovskite microwave ceramic system for $x = 0.04$, 0.06, 0.1, 0.3 and 0.5 was measured and evaluated to obtain the complex dielectric function and optical conductivity. Polar phonon parameters were determined, discussed and compared with those recently found for the conducting perovskite $LaTiO_3$. LTA $-$ x is a low loss high permittivity dielectric with no dispersion of permittivity between 10^9 and 10^{12} Hz range. In this range the dielectric losses increase roughly proportionally to frequency, as expected from the theory. This fact together with the low value of the losses indicates that the extrinsic losses were mainly suppressed during the processing and the remaining microwave losses are predominantly intrinsic

Keywords: Infrared; Dielectric; MW ceramics

1. Introduction

$La_{2/3}TiO_3$ (LT) became potentially an interesting dielectric material after it was stabilized by a small amount of Al_2O_3 [1,2]. Subsequent research revealed that complete stabilization of its perovskite structure can be achieved by addition of at least 4 mol% $LaAlO_3$ (LA) [2]. Smaller amount of LA caused the appearance of multiphase ceramics comprising in addition to perovskite $La_{2/3}TiO_3$ also $La_2Ti_2O_7$ and $La_4Ti_9O_{24}$. Stabilized LT has the orthorhombic perovskite structure with a doubled unit cell along the c-axis. By increasing the LA content, the system remains single phase and the orthorhombic structure changes via tetragonal (for more than 10 mol% of LA) and simple cubic (≥ 20 mol% LA) into rhombohedral one (≥ 85 mol% LA) [2]. However, the resolution of the X-ray diffraction (XRD) technique used was not high enough to assure a definite interpretation of the cubic reflections. As suggested in reference [2], different inhomogeneous submicrometer structural arrangements are also possible.

Initial microwave (MW) dielectric measurements of stabilized LT (LTA $-$ x system) were performed by Negas et al. [1] who suggested this system as a prospective one for high permittivity MW resonators. More extensive MW study of this system was recently carried out by Suvorov et al. [3,4]. The influence of various sintering temperatures (1300–1450°C for 33 h) and atmospheres (air, oxygen) was investigated on 11 samples from 2 to 50 mol% of LA ($x \in (0.02, 0.5)$). It was shown that maximum permittivity ($\varepsilon' \approx 72$) can be reached for 4 mol% of LA ($x = 0.04$). On increasing content of LA the permittivity gradually decreases (to $\varepsilon' \approx 34$ for 50 mol% of LA) as well as dielectric losses. The temperature coefficient τ_f of the resonant frequency changes from positive to negative values crossing zero close to 30 mol% of LA (LTA $-$ 0.3). Particularly, this composition with $\varepsilon' = 45$ and quality $Q = \varepsilon'/\varepsilon''$ times frequency f factor $Q \cdot f = 33$ THz compares well with the best known MW ceramics [4,5].

The question may arise if the Q values so far reached [4] represent the lowest loss limit for this system of materials. During the recent years we have demonstrated [5,6] that for answering this question, infrared

* Corresponding author.

0921-5107/98/$ - see front matter
PII S0921-5107(98)00252-9

(IR) reflectivity combined with submillimetre (SMM) and near-millimetre (NMM) transmission measurements is a very useful tool. Namely, from these data it can be estimated whether the losses are purely intrinsic, i.e. caused by inevitable multiphonon absorption (present even in a defect-less single crystal) or not. In the former case the simple proportionality $\Delta\varepsilon''_{\rm ext}(f) \propto f$ is expected for frequency f much smaller than all polar phonon eigenfrequencies (smaller than the averaged damping of thermally activated phonons) and the temperature higher than the Debye temperature. Most of the extrinsic contributions, however, also obey the proportionality $\Delta\varepsilon''_{\rm ext}(f) \propto f$ so that temperature dependences of IR and NMM losses and extrapolation from the one-phonon absorption region are needed to estimate the $\varepsilon''_{\rm int}$ and $\Delta\varepsilon''_{\rm ext}$ contributions.

In this paper we present first results of room-temperature IR reflectivity and NMM transmission measurements and their careful evaluation for five compositions (LTA − 0.04, 0.06, 0.1, 0.3, 0.5). The phonon parameters are evaluated and discussed and from the extrapolation of losses it is shown that the MW losses in the whole system studied are essentially intrinsic.

2. Experimental

The ceramic samples were prepared by standard solid-state reaction technique from highly purified La_2O_3, TiO_2 and Al_2O_3 as described in [4]. The resulting density was better than 97% of the theoretical value. For all the samples, the MW dielectric properties were determined using the resonant cavity method [4]. For IR reflectivity measurements, the sintered pellets of ~8.5 mm in diameter were single-side polished to obtain a flat lustrous surface. For NMM transmission measurements various double-side polished plane-parallel disks of thickness 0.2–0.7 mm were prepared. The reflectivity measurements were carried out using a standard Fourier transform Bruker IFS 113v spectrometer in the 30–3000 cm^{-1} spectral range. The transmission measurements were performed with a home-made monochromatic spectrometer 'Epsilon' (Inst. Gen. Phys., Moscow) [7] using tunable backward wave oscillators as sources in the 6–20 cm^{-1} range. The transmittance spectrum consists of interference maxima whose frequency positions determine the real part of the permittivity and the transmittance value at these maxima determine the dielectric loss (imaginary part of the permittivity) [5–7].

3. Results and evaluation

In Fig. 1 we present the room-temperature reflectivity spectra of our ceramics in the relevant frequency range below 1000 cm^{-1}. Above 1000 cm^{-1} no one-phonon absorption was observed and the ceramics became semi-transparent; therefore, due to the multiple beam reflection the corresponding reflectance values are higher than the actual ones should be and were not used for the fitting procedure. For the fitting procedure the generalized four-parameters damped oscillator model was used, which is known to give the best results in the case of broad and strong reflectivity bands [8]:

$$R = \left|\frac{\sqrt{\hat{\varepsilon}}-1}{\sqrt{\hat{\varepsilon}}+1}\right|^2$$

$$\hat{\varepsilon} = \varepsilon_\infty \prod_{i=1}^{n} \frac{\omega_{{\rm L}i}^2 - \omega^2 + i\omega\gamma_{{\rm L}i}}{\omega_{{\rm T}i}^2 - \omega^2 + i\omega\gamma_{{\rm T}i}} \quad (1)$$

where ε_∞ is the high frequency optical permittivity, $\omega_{{\rm T}i}$ and $\omega_{{\rm L}i}$ denote the transverse and longitudinal angular frequencies of the ith polar mode and $\gamma_{{\rm T}i}$ and $\gamma_{{\rm L}i}$ denote their respective damping constants. Six or seven oscillators were used to fit the most pronounced spectral features (see the dotted lines in Fig. 1) and the corresponding parameters are listed in Table 1. For each couple of transverse and longitudinal frequencies its dielectric strength was calculated from the formula [8]:

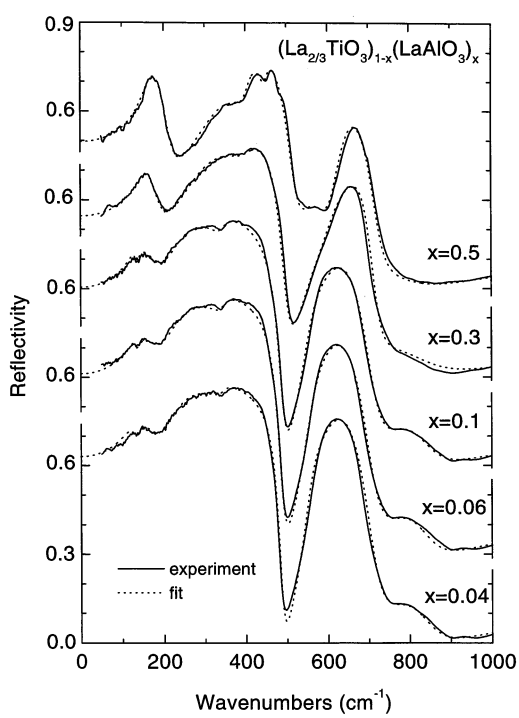

Fig. 1. Room temperature reflectivity spectra (solid lines) and their fits (dotted lines) of the LTA − x system for different compositions.

Table 1
Fitted mode parameters of the LTA$-x$ system for different compositions

x	0.04	0.06	0.1	0.3	0.5
ω_{T1}	131.72	130.74	130.83	—	—
γ_{T1}	34.23	21.03	12.39	—	—
ω_{L1}	131.93	132.08	131.90	—	—
γ_{L1}	20.78	16.56	9.55	—	—
$\Delta\varepsilon_1$	1.69	4.68	3.73	—	—
ω_{T2}	138.01	144.81	144.27	154.12	164.08
γ_{T2}	50.78	53.84	53.25	47.16	38.16
ω_{L2}	177.72	175.26	178.24	186.80	214.94
γ_{L2}	83.59	79.19	77.20	62.33	59.96
$\Delta\varepsilon_2$	44.22	30.75	30.75	18.95	17.29
ω_{T3}	224.79	223.84	232.10	281.95	326.33
γ_{T3}	79.50	84.25	89.88	119.77	127.76
ω_{L3}	343.09	341.97	339.63	399.36	400.19
γ_{L3}	46.78	46.78	49.67	74.42	58.75
$\Delta\varepsilon_3$	23.49	25.29	23.00	18.88	10.17
ω_{T4}	343.72	343.32	341.97	402.01	405.03
γ_{T4}	42.88	42.43	45.33	68.37	43.01
ω_{L4}	488.11	489.57	491.01	499.47	520.06
γ_{L4}	21.49	27.89	30.71	39.65	53.90
$\Delta\varepsilon_4$	0.07	0.16	0.28	0.19	0.41
ω_{T5}	—	—	—	—	449.62
γ_{T5}	—	—	—	—	23.02
ω_{L5}	—	—	—	—	447.91
γ_{L5}	—	—	—	—	25.55
$\Delta\varepsilon_5$	—	—	—	—	0.07
ω_{T6}	555.53	557.88	553.84	559.24	552.39
γ_{T6}	39.40	47.87	53.25	94.07	89.02
ω_{L6}	591.15	589.41	590.86	578.62	590.53
γ_{L6}	172.68	167.17	200.16	101.63	74.49
$\Delta\varepsilon_6$	1.11	1.07	0.92	0.73	0.37
ω_{T7}	592.87	590.86	597.97	597.58	624.14
γ_{T7}	132.55	138.84	153.29	88.03	56.79
ω_{L7}	713.86	709.98	712.41	717.39	722.94
γ_{L7}	70.93	70.24	71.57	49.92	58.32
$\Delta\varepsilon_7$	0.06	0.05	0.18	0.81	0.44
ω_{T8}	783.23	783.05	783.09	727.54	757.71
γ_{T8}	156.92	153.75	151.88	190.02	218.03
ω_{L8}	851.67	849.31	850.72	843.48	810.62
γ_{L8}	123.96	112.00	127.92	234.30	204.43
$\Delta\varepsilon_8$	0.20	0.21	0.21	0.08	0.09
ε_∞	5.0	5.0	4.9	4.7	4.5
$\varepsilon_o = \varepsilon_\infty + \Sigma\,\varepsilon_j$	75.8	67.2	64.0	44.3	33.3

ω_T, ω_L, γ_T and γ_L expressed in cm^{-1}, see text for the meaning of the parameters.

$$\Delta\varepsilon_i = \varepsilon_\infty \frac{\prod_j (\omega_{Lj}^2 - \omega_{Ti}^2)}{\omega_{Ti}^2 \prod_{j\neq i} (\omega_{Tj}^2 - \omega_{Ti}^2)} \quad (2)$$

The calculated dielectric function (using Eq. (2)) was extrapolated beyond the low-frequency end of the reflectivity spectra and compared with that calculated from NMM transmission and MW measurements. We tried to optimize the fit simultaneously in the IR and NMM range and the resulting complex dielectric function together with the NMM and MW experimental data is shown in Fig. 2. The ε_∞ values, which do not influence significantly the fit below 1000 cm^{-1}, are independently known for pure LA only ($\varepsilon_\infty = 4$ [9]). The high-frequency reflectivity data indicate that for the $x = 0.04$ sample the best fit value is about $\varepsilon_\infty = 5$. For the remaining samples we use rounded interpolated values as indicated in Table 1.

In Fig. 3 we show the optical conductivity $\sigma(\Omega^{-1}\,cm^{-1}) = 1.664\cdot 10^{-2}\ \varepsilon''\omega\ (cm^{-1})$ [10] plotted in the linear frequency scale which shows in the best way the transverse polar phonon mode response. The area under each conductivity peak is proportional to its oscillator strength or to the mode effective charge squared and the integral over the whole conductivity spectrum obeys the oscillator strength sum rule [10].

In Fig. 4 we have plotted the fitted transverse and longitudinal phonon frequencies as a function of composition. Six couples of modes are present for all the compositions. One additional couple is present in the low-frequency range near 130 cm^{-1} for $x = 0.04$, 0.06 and 0.1, and another one near 450 cm^{-1} for the $x = 0.5$ sample.

4. Discussion

Let us first discuss the polar phonon parameters. Three loss peaks (modes 2, 3 and the overlapping couple 6 + 7 in Table 1) dominate in all dielectric (or conductivity) spectra. These peaks can be assigned to the three IR active modes of the prototypic simple cubic perovskite structure [11]. The additional weaker spectral features can be assigned to modes activated due to the unit cell doubling [2] (in the case of $x = 0.04$, 0.06 and 0.1) or due to higher concentration of LA (in the case of $x = 0.3$ and 0.5) which may allow formation of some structural clusters, even if the averaged simple cubic structure comprises only one formula unit in the unit cell like the pure LA. This qualitatively agrees with the conclusions from the XRD data [2] mentioned in the introduction.

Comparison with the three main transverse mode frequencies in pure LA [9] shows that in the LTA solid solution the behaviour of all three modes is essentially that of one-mode type [12] where the main ω_T frequencies shift with the composition continuously from about 138, 225 and 556 cm^{-1} for hypothetical LT to 184, 428 and 652 cm^{-1} for LA, respectively. In the case of the highest frequency mode this statement is not that clear and for the $x = 0.5$ sample, some features of the two-mode behaviour are apparent (Fig. 3) which was taken into account in our fit for all the compositions (modes 6 and 7).

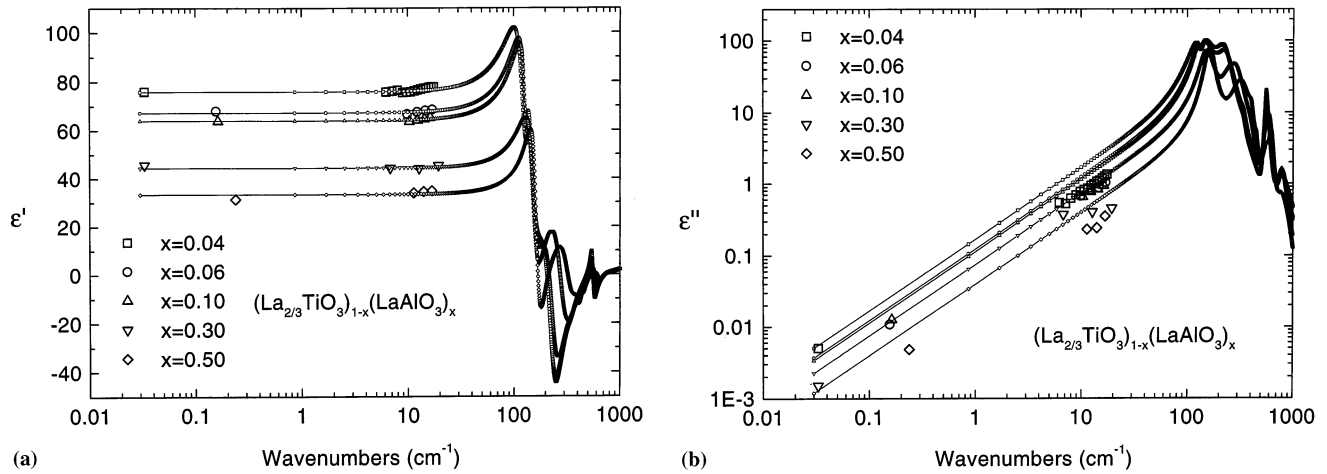

Fig. 2. Dielectric function of the LTA – x system for different compositions, calculated from the fit to reflectivity in Fig. 1 together with experimental NMM and MW points: real (a) and imaginary (b) parts.

The comparison of Fig. 3 with the polar phonon spectrum of LA [9], where the assignment of all three main modes is more or less clear [13], allows us to discuss qualitatively the main mode assignment in our spectra. The highest-frequency mode, like in all perovskite-like structures, corresponds to oxygen octahedra bending [14]. The intermediate mode in the LA case is predominantly of Al–O_6 stretching type and the lowest-frequency one external La–BO_6 octahedra translation. On increasing Al → Ti substitution, the intermediate mode softens rapidly which indicates its hybridization with the lowest external mode. This is in agreement with the well known fact that in ferroelectric titanates the Ti–O_6 stretching mode plays the role of the lowest-frequency ferroelectric soft mode [14]. In our case of small x compositions, the ferroelectric instability is not yet reached so that both low-frequency modes are strongly hybridized, i.e. their frequencies are rather close and their dielectric strengths are rather high.

The most surprising fact seems to be that the La vacancies in the small x samples do not manifest themselves in the spectra in any striking way, but only by

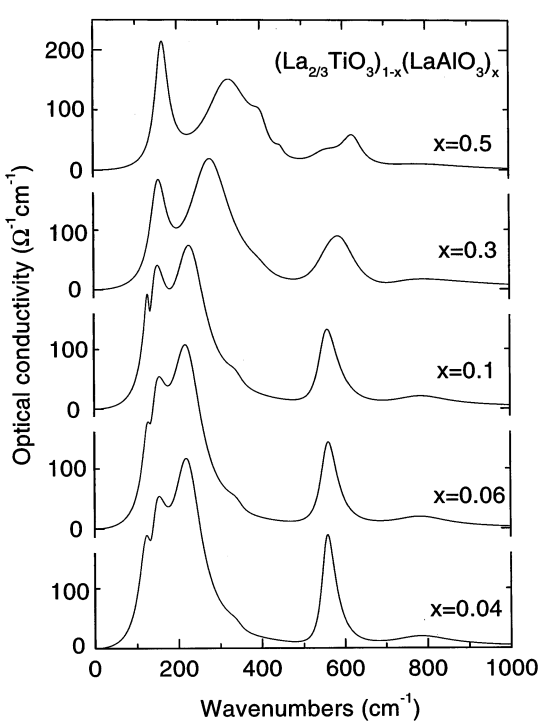

Fig. 3. Optical conductivity of the LTA – x system for different compositions calculated from the reflectivity fit.

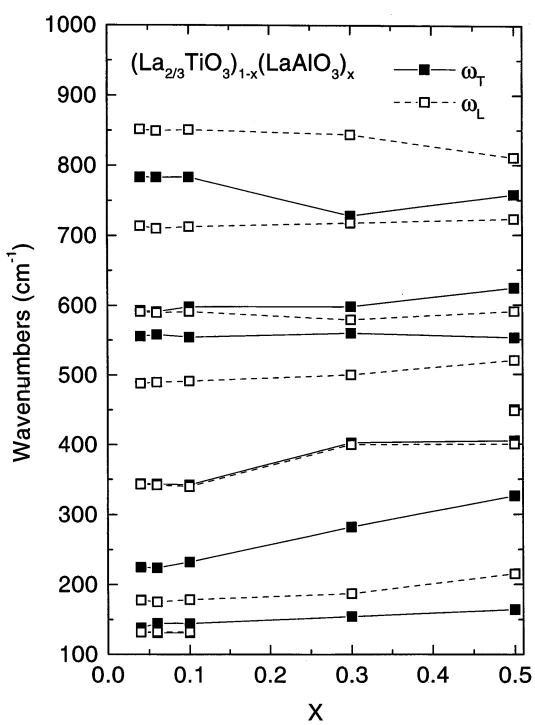

Fig. 4. Dependence of the transverse (ω_T) and longitudinal (ω_L) polar frequencies on the composition x in the LTA – x system.

Table 2
Comparison of the dielectric permittivity and losses of the LT–LA ceramics extrapolated from the fit to IR data and directly measured in the NMM and GHz range

x	ε'			$Q \cdot f$ (THz)		
	MW	NMM	IR	MW	NMM	IR
0.04	76.0	76.4	75.8	16.1	30.1	13.6
0.06	68.0	67.7	67.2	29.5	31.6	16.4
0.1	63.8	64.3	64.0	24.7	32.5	17.0
0.3	45.7	44.6	44.3	30.5	38.9	17.9
0.5	34.4	34.4	33.3	45.0	54.1	25.3

The NMM values are averaged over the measured range (Fig. 2).

decrease in mode frequencies, which is stronger that one could expect from the mass effect from Al (a.m. 27) to Ti (a.m. 47.9). This shows that in force constants determining the long-wavelength polar lattice dynamics, the long-range contribution prevails and so averages over the local density fluctuations due to the La vacancies. It would be of interest to investigate the effect of such local inhomogeneities on the short wavelength lattice dynamics, concerning the phonons away from the centre of the Brillouin zone.

It is interesting to compare our IR spectra of $La_{2/3}TiO_3 + 0.04$ $LaAlO_3$ with those of a semimetallic $LaTiO_3$ (with three-valent Ti^{3+} ions) which also crystallizes in the (slightly orthorhombically distorted) perovskite structure [15]. In the latter case the conductivity spectrum is strongly influenced by a heavily damped Drude and mid-IR electronic contribution, but the phonon parameters still can be well determined from the fit to the IR reflectivity. Also in this case three phonon modes (near 170, 340 and 545 cm^{-1}) dominate the spectrum. It is seen that whereas the highest frequency mode has frequency comparable to that in $LT - 0.04$, both lower frequencies are much higher than in LT. This might be expected since the La^{3+} ions are obviously more weakly bound in the LT lattice (due to the La vacancies) than in the $LaTiO_3$ one.

Let us now discuss the lower-frequency NMM and MW range. From Table 1 and Fig. 2 it is clear that the ε' values extrapolated from the IR range agree perfectly (within the limits of experimental accuracy) with the measured NMM and MW values. It means that there is no appreciable dielectric dispersion below the IR range and the MW permittivity value ε' (MW) is fully composed of polar phonon contributions plus ε_∞ (Tables 1 and 2). This is a usual case for weakly anharmonic crystals and well processed ceramics with not too high permittivity ($\varepsilon' \leq 100$) [5,6].

The discussion of low-frequency losses is much more delicate because the losses become very small in the MW range in comparison with those in the IR range (Fig. 2) and therefore they become much more sensitive to all imperfections [5,6]. Moreover, the extrapolation of the simple damped harmonic oscillator model to two to four orders of magnitude lower frequencies is highly questionable from the theoretical point of view even in a defect-less single crystal [5,16,17], but the order of magnitude of the extrapolation loss agrees with that directly measured in most of the well processed single-phase ceramics investigated [6].

In reference [5] we already listed some of our preliminary data concerning this comparison and it was demonstrated that the LTA system belongs to a rare case where the extrapolation from the IR range yields higher losses than those directly measured in the NMM and MW range. This is also clearly seen in Fig. 2(b) and in Table 2 where the numerical $Q \cdot f$ values are summarized. The $Q \cdot f$ values measured in NMM and MW range agree with each other within the limits of experimental accuracy, but are somehow higher than those obtained from the IR oscillator model. Trial fits (including the model of classical oscillators [5]) have demonstrated that this fact is clearly outside the experimental errors and brings evidence that in the low-frequency region the constant oscillator damping approximation (which follows from Eq. (2)) is not sufficiently well fulfilled. The poor present state of knowledge of the lattice dynamics in the LTA system does not allow us to speculate about the microscopic reason for it, but it may be expected theoretically for low and intermediate permittivity crystals [17]. Nevertheless, the low values of NMM and MW losses bring a strong argument in favour of the prevailingly intrinsic origin of the losses because extrinsic losses would show up mostly by the increased loss in the MW range.

It should be noticed that one extrinsic loss source is inherently present in all solid solutions: due to the broken lattice periodicity the selection rules for one-phonon absorption based on quasi-momentum conservation are relaxed and all the phonons become slightly IR active. This results in a weak absorption background roughly proportional to the one-phonon density of states which in the low-frequency range (where only acoustic phonons contribute to the density of phonon states) yields $\Delta\varepsilon'' \propto f$, like the intrinsic loss contribution [5,6,16]. The fact that our $Q \cdot f$ values are constant in the 10^9–10^{12} Hz range is in agreement with these predictions, but does not allow us to separate both loss contributions mentioned. This could be done only from low-temperature loss data where the intrinsic two-phonon losses should vanish whereas the extrinsic contribution is expected to be temperature independent. Such experiments are scheduled for our next work.

5. Conclusions

Unlike conducting $LaTiO_3$, stabilized $La_{2/3}TiO_3$ system is a high permittivity dielectric with no dispersion of

the permittivity between 10^9–10^{12} Hz. Evaluation of the IR reflectivity enabled us to determine the polar mode parameters in the LTA $-x$ system. The main three modes present in all five LTA $-x$ compositions were assigned. Comparison with the polar modes in $LaTiO_3$ shows that the $x = 0.04$ ceramic has much lower eigenfrequencies of the polar vibrations where the La ions take part, which is the only manifestation of La vacancies in the latter case. This shows on the important role of the long-range interatomic forces which control the normal mode eigenfrequencies. Below the polar phonon frequencies, the near-millimetre dielectric losses are lower than those extrapolated from the oscillator fit to IR reflectivity. Nevertheless the losses are proportional to frequency in the range of at least 10^9–10^{12} Hz. This shows that the losses in this range are predominantly of intrinsic two-phonon absorption origin and the samples have their microwave losses essentially minimized.

Acknowledgements

The authors thank S. Kamba for helpful discussions. The work was supported by the Grant Agency of the Czech Republic (project no. 202/98/1282), by Czech Ministry of Education (project Kontakt ME-100) and partially by the Russian Foundation for Basic Research (grant no. 96/02/17350). One of us (E. B.) was supported by the Government of the Basque Country, Spain, (PhD scholarship of the program 'Formación de investigadores del Departamento de Educación, Universidades e Investigación').

References

[1] T. Negas, G. Yeager, S. Bell, R. Amren, Chemistry and properties of temperature compensated microwave dielectrics, in: P.K. Davies, R.S. Roth (Eds.), Proc. Int. Conf. Chemistry of Electronic Materials, Jackson, (NIST SP 804), August 1990, p. 21.
[2] S. Škapin, D. Kolar, D. Suvorov, J. Am. Ceram. Soc. 76 (1993) 2359.
[3] D. Suvorov, D. Kolar, Ferroelectrics 154 (1994) 253.
[4] D. Suvorov, M. Valant, S. Škapin, D. Kolar, J. Mater. Sci. 33 (1998) 85.
[5] J. Petzelt, S. Kamba, G.V. Kozlov, A.A. Volkov, Ferroelectrics 176 (1996) 145.
[6] J. Petzelt, N. Setter, Ferroelectrics 150 (1993) 89.
[7] A.A. Volkov, Yu.G. Goncharov, G.V. Kozlov, S.P. Lebedev, A.M. Prokhorov, Infrared Phys. 25 (1985) 369.
[8] F. Gervais, Infrared and millimetre waves, in: K.J. Button (Ed.), High-Temperature Infrared Reflectivity Spectroscopy by Scanning Interferometry, ch. 7, vol. 8, Academic Press, New York, 1983, p. 279.
[9] Z.M. Zhang, B.I. Choi, M.I. Flik, A.C. Anderson, J. Opt. Soc. Am. B 11 (1994) 2252.
[10] P. Brüesch, in: P. Fulde (Ed.), Phonons: Theory and Experiments II, Springer Series in Solid-State Sciences 65, Springer, Berlin, 1986.
[11] M.E. Lines, A.M. Glass, Principles and Application of Ferroelectrics and Related Materials, Clarendon Press, Oxford, 1977.
[12] D.W. Taylor, Phonon response theory and the infrared and Raman experiments, in: R.J. Elliot, I.P. Ipatova (Eds.), Optical Properties of Mixed Crystals, Modern Problems in Condensed Matter Sciences, North-Holland, Amsterdam, 1988, p. 35.
[13] C.H. Perry, D.J. Mc Carthy, G. Rupprecht, Phys. Rev. 138A (1965) 1537.
[14] W. Kinase, Y. Ishibashi, K. Matsuura, J. Phys. Soc. Jpn. 19 (1964) 264.
[15] D.A. Grandles, T. Timusk, J.D. Garret, J.E. Greedan, Phys. Rev. B 49 (1994) 4229.
[16] V.L. Gurevich, A.K. Tagantsev, Adv. Phys. 40 (1991) 716.
[17] A.K. Tagantsev, J. Petzelt, N. Setter, Solid State Commun. 87 (1993) 1117.